SENRA Academic Publishers, Burnaby, British Columbia
Vol. 2, No. 2, pp. 451-458, 2008
ISSN: 1715-9997

Canadian Journal of pure&applied sciences

FEM SIMULATION WITH EXPERIMENTAL VERIFICATION OF SINTERED FORGED COMPONENTS

*Suprakash Patra[1], Goutam Sutradhar[2], Amitava Mandal[3]
[1]AWS, CWISS, Indian Institute of Technology, Kharagpur
[2]Department of Mechanical Engineering, Jadavpur University, Kolkata
[3]National Institute of Foundry and Forge Technology, Hatia, India

ABSTRACT

Powder metallurgy (P/M) is one of the most diverse approaches in metal forming. The main attraction of this process is the ability to fabricate high quality complex parts to close tolerances in an economical manner. Extensive research work has been done on this field. It has been reported by so many authors that if this process is properly performed the P/M products approaches to full density which belongs better mechanical response compare to their equivalent wrought materials, largely because of the microstructural homogeneity. In this present work P/M steel components were forged under cold condition and the predicted results were verified with the help of DEFORM-3D software package. The theoretical analysis and the FEM models agree the experimental results.

Keywords: Cold forging, iron powder, metal powder preform, simulation, FEM.

INTRODUCTION

Forging of Powder metallurgy (P/M) components deliver net shape parts having reliable dimensional tolerances and accurate chemical composition etc. several advantages over ordinary P/M components eliminating the machining operation increases material utilization. It was reported that this process leads to a net cost saving compared to the conventional approach under mass production and the P/M products approaches to full density which belongs better mechanical response compare to their equivalent wrought materials, largely because of the microstructural homogeneity, Ramakrishna (1980). Powder forged parts are used in connecting rods in US automobiles since 1987, which are superior than conventional products due to uniform microstructure and better material distribution. Now-a-days development of super plastic ceramic materials from ceramic perform has been developed for high bearing and seal applications.

The plastic deformation of powder particles during compaction promotes the mechanical interlocking which ultimately control the density and hardness (Haglund and Agren ,1998; German, 1994). The particle bonding is dependent on interatomic and electrostatic force at surface. The small size powder with clear surface has stronger force and irregular particle shape, enhance better mechanical interlocking between the particles (David *et al*., 1998; German, 1990). A substantial work has been done by the various workers Vedis and Geiling (1981), Sutradhar *et al*. (1994, 1995) on cold forging of sintered iron powder performs. Work has also been done on modeling on prediction of shrinkage Shama *et al*. (2002). It is needless to mention that there is an immense potential in this particular field. A lot of authors (Oozo and Yang, 1992; Ibhadode, 1989; Mori *et al.*, 1980; Im and Kobayashi, 1986; Oh *et al.,* 1987) have been reported the P/M forging by FEM analysis and simulation technique with the following assumptions.

- Elastic portion of deformation is neglected because, practical forging process involves very large amount of plastic deformation.
- The normality of the plastic strain rates to the yield surface holds.
- An-isotropic behavior, which occurs during deformation, is negligible.
- Thermal properties of porous material are independent of temperature.

Following observations have been made by the above authors, for small reduction, almost no change in relative density at the central region, as the reduction increases the relative density near the bulged free surfaces increases and the equatorial free surface is possible fracture site which was indeed by experience also. Substantial work has been reported by various authors on cold forging of sintered powder performs during last two decades. But no work has been published regarding the verification of Upper Bound method with the Simulation Software like Ausys or Deform-3D. For analysis the preform is divided into 1500 elements (Fig.1). Therefore, an attempt has been made to access the die load in two methods and which have been verified by experimental results.

*Corresponding author email: suprakashpatra@lycos.com

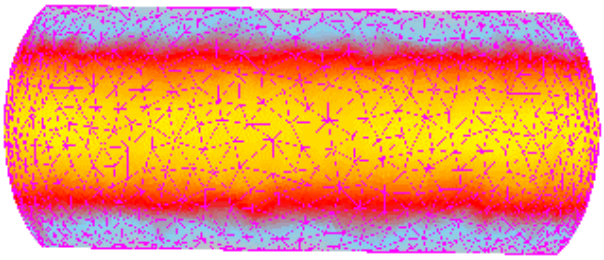

Fig. 1. Preform divided into 1500 elements.

Analysis by Upper Bound Method

In metal forming process friction condition between work piece and deforming tool is of most important and a number of factors such as force and mode of deformation, properties of the finished specimen and resulting surface roughness are the most deciding factors for the successfulness of the process. The relative velocity between the work piece material and the die surface together with high interfacial pressure and deformation modes will create the conditions essential for adhesion in addition to sliding.

Due to application of compressive hydrostatic stress in cold forging i, e, plastic deformation the pores will close and the relative density will increase, but in case of tensile hydrostatic stress the pores will grow and relative density will decrease. The density distribution is also not uniform. It is high at the central region and low at edges. The density will be more uniform for smaller coefficient of friction μ and for a greater initial density Tabata *et al.* (1980). During cold forging of metal powder preforms the compressive force gradually increases the relative density that is directly proportional to the real area of contact. The relative density gradually approaches the apparent relative density and this approach is asymptotic.

During the sinter cold forging processes it is very important to keep special consideration on interfacial friction, as this will determine the success or failure of the operation. The relative velocity between the workpiece material and the die surface, together with high interfacial pressure and deformation modes, create a condition of composite friction, which is due to the adhesion and sliding Deryagin *et al.* (1952). The sheer equation becomes $\tau=\mu\ (p+\rho_0\ \phi_0)$, the first term μp is due to the sliding and the second term $\mu\rho_0\ \phi_0$ being due to adhesion, which latter arises from chance of relative density of the pre-form during forging process.

The pattern of metal flow during the cold forging of a metal powder pre-form is such that there exists two zones, an inner where no relative movements between work piece and die occurs (the sticking zone) and an outer zone where sliding occurs. Therefore the appropriate friction laws for different conditions are:

Axisymmetric Conditions

$$\tau = \mu\,[\,p + \rho\,\varphi\{\,1-(\ \tfrac{r_m - r}{nr_0}\ )\}] \qquad (1)$$

Plain strain conditions

$$\tau = \mu[\,p + \rho_0\varphi_0\,\{1-(\tfrac{x_m - x}{nb})\}] \qquad (2)$$

r_m and x_m denote the radius of the sticking zone axisymmetric and plane strain conditions respectively, which may be approximated by the relationship given by Rooks (1974) and n>>1.

As it is a case of axisymmetric condition.

Velocity field and strain rates

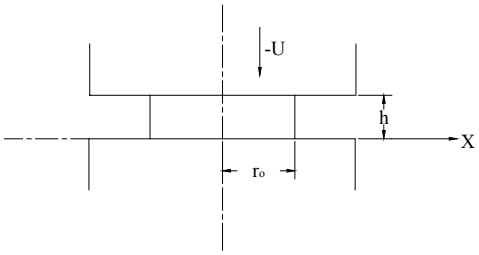

Fig.2. Forging of disc.

The velocity of the upper die is taken as $-\dot{U}$ as shown in Fig.2. The radial and axial velocity components $\dot{U}_r$ and $\dot{U}_z$ are assumed as

$$\dot{U}_r = \frac{(1-2\eta)\dot{U}}{2(1+\eta)h}\,r \qquad (3)$$

$$\dot{U}_z = -\frac{z\dot{U}}{h} \qquad (4)$$

$$\dot{U}_\theta = 0$$

The corresponding strain rates are

$$\dot{\varepsilon}_r = \frac{\delta \dot{U}_r}{\delta r} = \frac{(1-2\eta)\dot{U}}{2(1+\eta)h} \qquad (5)$$

$$\dot{\varepsilon}_\theta = \frac{\dot{U}_r}{r} = \frac{(1-2\eta)\dot{U}}{2(1+\eta)h} = \dot{\varepsilon}_r \qquad (6)$$

$$\dot{\varepsilon}_z = \frac{\delta \dot{U}z}{\delta z} = -\frac{\dot{U}}{h} \qquad (7)$$

The above normal-strain components satisfy the compressibility equation for the axisymetric condition for porous material.

$$\dot{\varepsilon} + \frac{(1\pm 2\eta)}{2(1\pm\eta)}\dot{\varepsilon} = 0 \quad \text{(Refer to Appendix)} \qquad (8)$$

For plastic deformation of a metal powder, the external power J^* supplied by the die is given as

$$J^* = \frac{2}{\sqrt{3}}\sigma_0 \int \sqrt{\tfrac{1}{2}} e_{ij} e_{ij}\, dV + \int_s \tau v I D s + \int_V \rho a_i U_i\, dV - \int_{st} T_i V_i\, ds \quad (9)$$

The first term on the right hand side denotes the rate of internal energy dissipation W_i the second term denotes the frictional shear energy losses W_f, the third term denotes the energy dissipation due to inertia forces W_o, and the last term covers power supplied by predetermined body tractions W_t. In this case forces due to inertia are negligibly small and no external surface traction is stipulated. Moreover forces due to inertia are negligibly small. Therefore $W_a = W_t = 0$.

The external power J^* supplied by the press through the piston is

$$J^* = W_i + W_f = P\dot{U} \quad (10)$$

The rate of energy dissipation per unit volume is given by

$$DW_i = \sigma_1\, d\varepsilon_1 + \sigma_2\, d\varepsilon_2 + \sigma_3\, d\varepsilon_3 \quad (11)$$

The total internal energy dissipation in the disc is

$$W_i = \frac{\rho^k \sigma_0 \dot{U}}{(1+\eta)} \pi b^2 \quad (12)$$

The rate of energy dissipation due to the friction W_f is given by

$$W_f = \int_s \tau |\Delta V| ds \quad (13)$$

Considering the magnitude of the relative velocity ΔV

$$\Delta V = \left|\dot{U}_r\right|_Z = 0, h^{-0} = \frac{(1-2\eta)r}{2(1+\eta)h} \quad (14)$$

$$ds = 4\pi r\, dr$$

$$W_f = \frac{2}{3} \frac{\pi\mu(1-2\eta)\dot{U}r_0^3}{(1+\eta)h}\left[\rho_{av} + \rho_0\phi_0\left\{1 + \frac{3}{4n} - \frac{r_m}{nr_0}\right\}\right] \quad (15)$$

Die Load

Using the equations

$$PU = \frac{\rho^k \sigma_0 U \dot{\pi r_0}^2}{(1+\eta)} + \frac{2}{3} \frac{\pi\mu(1-2\eta)\dot{U}r_0^3}{(1+\eta)h}\left[\rho_{av} + \rho_0\phi_0\left\{1 + \frac{3}{4n} - \frac{r_m}{nr_0}\right\}\right] \quad (16)$$

$$P_{av} = \frac{P}{\pi r_0^2}, \text{ for } \rho_0\varphi_0 = 0.3\, p_{av} \quad (17)$$

$$PU = \frac{\rho^k \sigma_0 U \dot{\pi r_0}^2}{(1+\eta)} + \frac{2}{3} \frac{\pi\mu(1-2\eta)\dot{U}r_0^3}{(1+\eta)h}\left[\frac{P}{\pi r_0^2} + \frac{0.3P}{\pi r_0^2}\left\{1 + \frac{3}{4n} - \frac{r_m}{nr_0}\right\}\right] \quad (18)$$

$$P = \left[1 - \frac{2r_0\mu(1-2\mu)}{3(1+\eta)h} - \frac{0.2\mu(1-2\eta)r_0}{(1+\eta)h}\left(1 + \frac{3}{4n} - \frac{r_m}{nr_0}\right)\right]^{-1} \frac{\rho^k \sigma_0 \pi r_0^2}{(1+\eta)} \quad (19)$$

For $0<x<1$ where $\rho_0\varphi_0 = xp_{av}$. and $n>>1$.

Experimental Work

Automised iron powder of purity 98% and finer than 150 μm was used. The sieve analysis of iron powder is as follows:

Screen Size (micron)	-150 +150	-106 +106	-75 + 75	-63 +63	-45 +45
Weight of the powder (%)	2 38	12.5	8.5	21.5	17.5

Apparent Density = 3.9 gm/cc.
Tap Density = 4.3 gm/cc.

Chemical Analysis of Iron Powder used.

C	Si	Mn	S	P	Fe
0.12	0.35	0.15	0.43	0.03	Balance

Compacting Pressure = 25 – 30 Kg./mm^2
Platen Speed = 1 mm/Sec.

Iron powder was compacted in a closed circular die. The die wall was lubricated with graphite. The compaction pressure of 25-30 Kg./mm^2 was maintained at 1000 psi (6.89 k Pa) and fifteen green compacts were prepared. These compacts were sintered in an argon atmosphere at about 1050^{o}C temperature for 2 hours in a horizontal Tubular furnace of maximum temperature capacity 1450 $\pm$ 1^{o}C. In order to minimize the non-uniformity of density distribution, the sintered compacts were re-pressed at the same compaction pressure in the same die and the specimens re-sintered. The average relative density of the re-sintered performs was found to be 0.70 to 0.80. The pre-forms were machined to the dimensions of diameter 12.7mm and 27.2 mm and different heights as shown in the tables. The surfaces of the specimens were polished with fine emery paper.

Table 1. Diameter 27.2, Height 11.4, RD 0.8, TD (f) 0.25, BD (f) 0.30

Red. %	Change in Hit. mm.			Load (N)		Top Dia(mm)		Middle Dia.(mm)		Bottom Dia.mm	
	Actual	Step	Sim.	Actual	Sim.	Actual	Sim.	Actual	Sim.	Actual	Sim.
12	1.368	17	1.36	224525	299058	27.70	28.013	28.80	28.291	28.00	27.90
24	2.888	36	2.88	343350	428177	28.54	29.382	30.40	29.986	28.80	29.12
32	3.65	46	3.68	490500	516592	30.00	30.373	31.11	31.152	29.95	30.03

Table 2. Diameter 12.7, Height 13.2, RD 0.7, TD (f) 0.50, BD (f) 0.55

Red. %	Change in Hit.(mm)			Load(N)		Top Dia. mm		Mid. Dia.(mm)		Bottom Dia.mm	
	Actual	Step	Sim.	Actual	Sim.	Actual	Sim.	Actual	Sim.	Actual	Sim.
30	3.96	49	3.92	96138	69957	13.54	13.62	14.52	14.38	13.40	14.32
42	5.54	69	5.52	100062	100331	13.92	13.89	15.70	15.90	13.90	13.78
55	6.52	83	6.64	117720	125232	14.50	14.054	16.92	16.40	14.65	14.043

Table 3. Diameter 12.7, Height 12.6, RD 0.8, TD(f) 0.25, BD(f) 0.3

Red. %	Change in Hit.(mm)			Load(N)		Top Dia.mm		Mid. Dia.(mm)		BottomDia.(mm.)	
	Actual	Step	Sim.	Actual	Sim.	Actual	Sim.	Actual	Sim.	Actual	Sim.
21.36	2.69	33	2.64	343350	378108	28.7	28.813	29.6	29.415	28.45	28.483
22.70	2.86	36	2.88	343350	396558	28.12	29.052	29.4	29.681	28.25	28.666
30.76	3.875	49	3.92	490500	490992	30.10	30.079	31.1	31.004	29.60	29.683

Following this the specimen was placed between lower and upper platens in both dry and lubricated conditions. Silicon grease is used as lubricant. The top diameter, middle diameter, and lower diameter and reduction in height were measured at various stages of compression and the loads were recorded. The upper platen moved at a speed of 1 mm/sec. The lower platen was held stationary. The results obtained are shown in the tables.

Simulation of Cold Forging of Metal Powder Preform

The simulations are carried out using software package DEFORM 3D. The pre-form is considered as porous and dies are considered as rigid. The elastic deformation is neglected. For analysis the per-forms are divided into 15000 elements.

The ambient temperature is selected as 20°C. The bottom die is fixed and top die is moving with the speed of 1 mm/sec. The heat exchange between work piece and dies and between the dies and ambient surrounding is incorporated in FEM calculation. The friction factor for pre-form and top die is calculated as 0.25 and for pre-form and bottom die as 0.30 in lubricated condition. The friction factor for un-lubricated case is calculated as 0.50 for top die and 0.55 for bottom die. The values of friction factors are assumed initially and then for one case these values are adjusted to give the observed dimensions of the pressed cylinder. Using these values for all the other cases gave good results.

The stress-strain curve for the powder material is shown in figure 3.

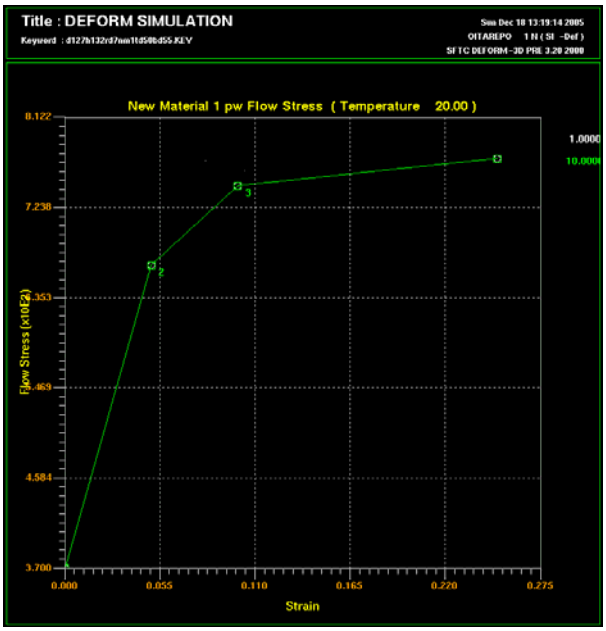

Fig. 3. Stress-strain curve of the iron powder used in the experiment.

The experimental results and simulation results are given in a tabular form.

TD(f) = the coefficient of friction value between top die and work-piece

BD(f) = the coefficient of friction value between bottom die and work-piece

RD = the relative density of pre-form.

Red. % = reduction in percentage of the height of original preform

Sim. Means results obtain after FEM simulation.

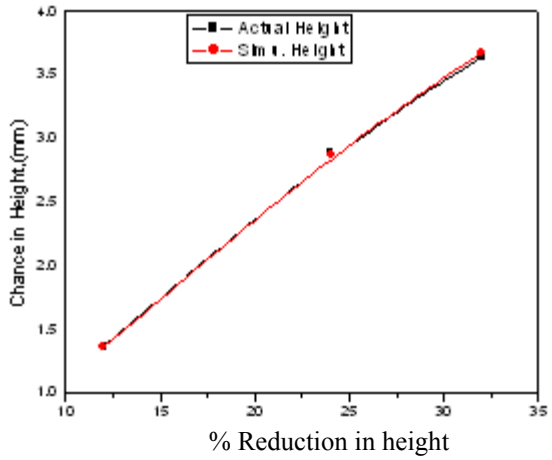

Fig. 4. Actual height reduction & Sim. Height reducation against % height reduction for Table 1.

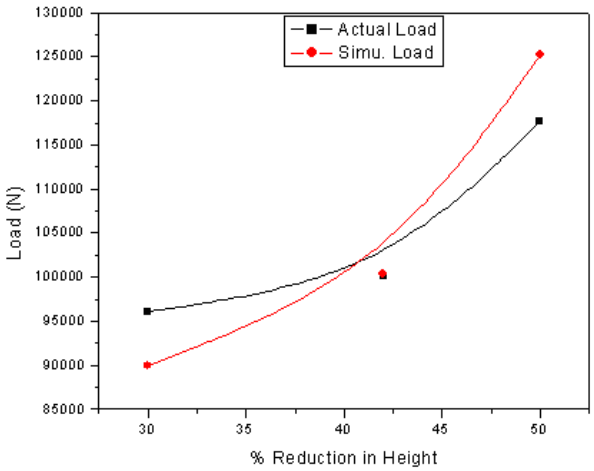

Fig. 5. Actual load & Sim. Load against % reduction height for Table 1.

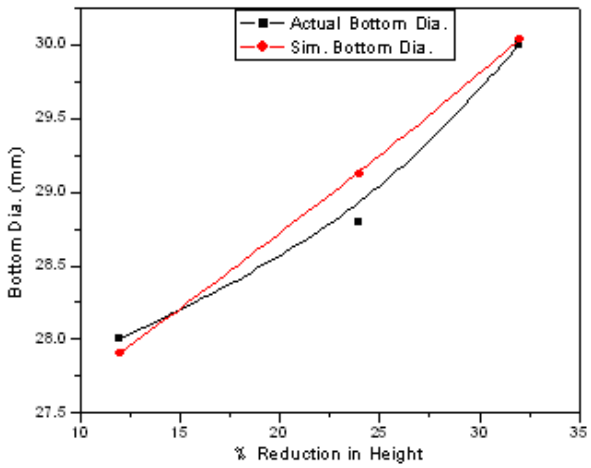

Fig. 6. Actual bottom dia. & Sim. dia against % reduction in height for Table 1.

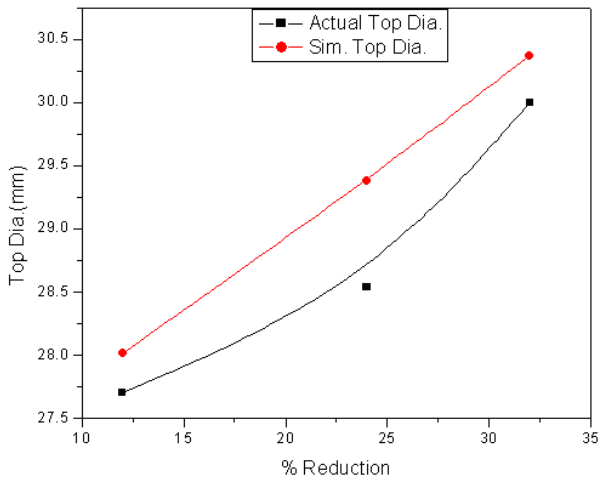

Fig. 7. Actual top dia. & sim. top dia. against % reduction in height for Table 1.

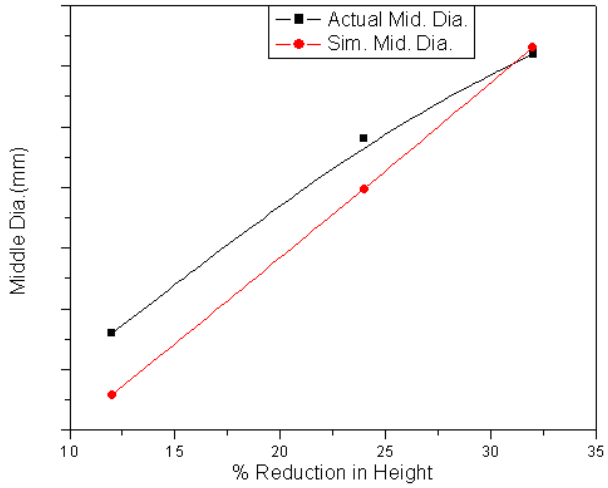

Fig. 8. Actual middle dia. & sim. middle dia. Against & reduction in height for Table 1.

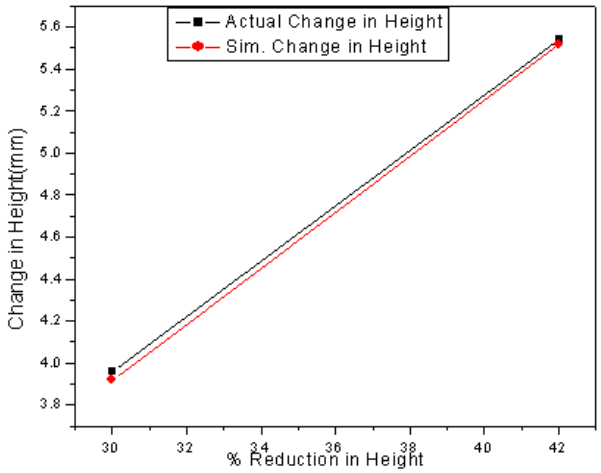

Fig. 9. Actual change in height against sim. change in height for particular % reduction in height for Table 1.

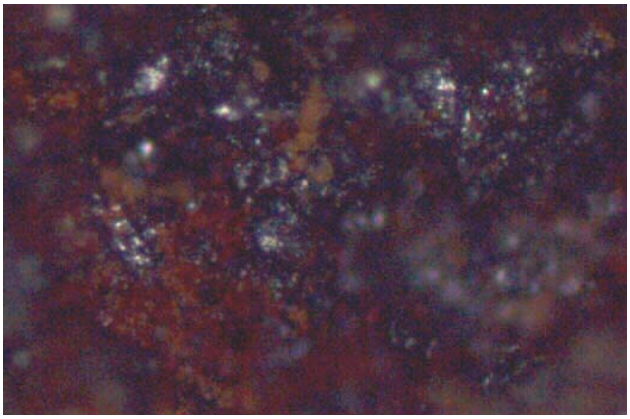

Fig. 10. Dense powder particles at center.

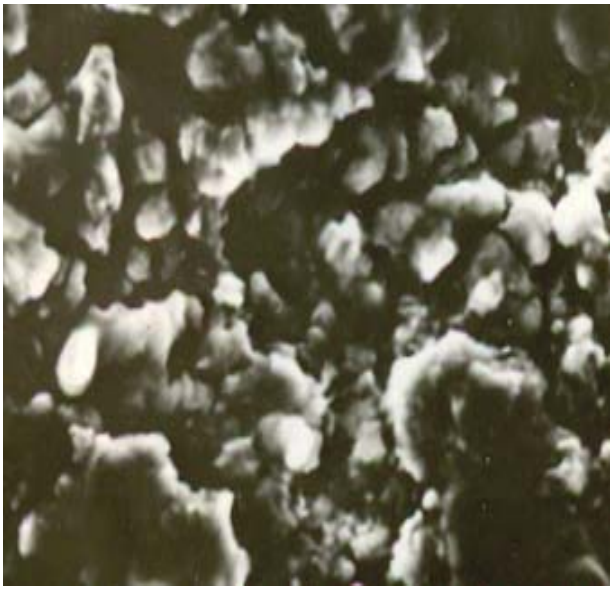

Fig.11. Powder Particles at the middle of sample.

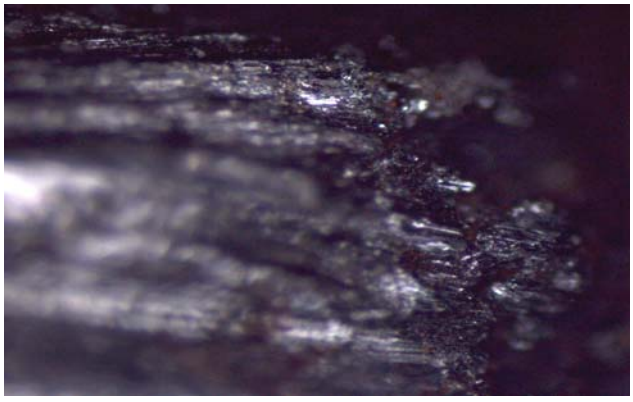

Fig. 12. Cracks formed at the bulging edge of sample

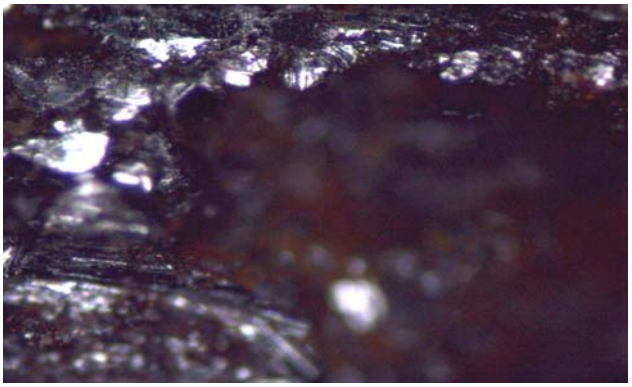

Fig. 13. Single crack (Enlarged view)

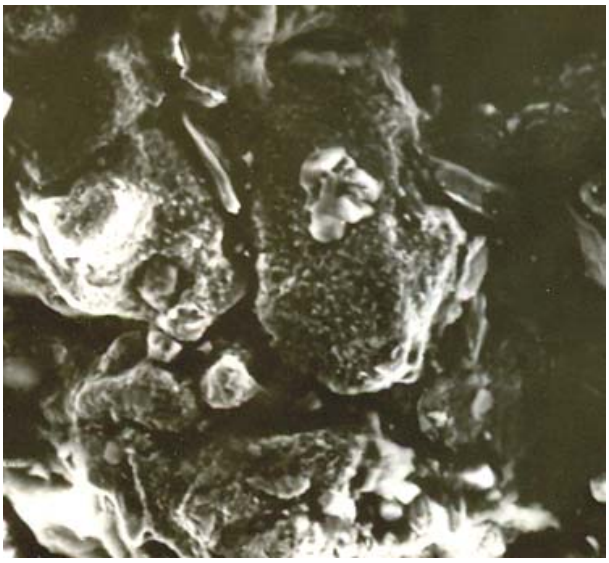

Fig. 14. Powder Particles at the edge of the sample.

RESULTS AND DISCUSSION

The results obtained from the experiments and from finite element based simulation are shown in tables 1-3. From the tables it is observed that at any percentage reduction in height the calculated load is close to the actual load recorded taking into consideration the low sensitivity of the machine used. The diameters of the cold forged performs at top, middle and bottom obtained through simulation at various stages are also quite close to the actual dimensions obtained from experiments. Which are shown in Figures 4-9.

A few cold pressed specimens were cut vertically and photographs were taken. The trends of relative density variation obtained from the photographs after analyzing them using SEM (Fig.10-14). It is clearly visible from the figure that the density is highest at the center and it gradually decreases towards the edges. Figure15 shows the variation of relative density with reduction in height for three points as obtained from FE simulation. The

calculated relative density is also more at the center for lubricated case than for un-lubricated case. Two samples were pressed till the crack appeared (Fig.12 and 13). The cracks are located at the middle of bulged portion. The simulation results (Fig.16) show that the relative density is minimum at those locations where cracks appeared.

CONCLUSIONS

FEM modal is a convenient tool for the prediction of density distribution and change in dimensions with reduction in height of the specimens at a particular time and boundary conditions. The friction factor calculated is 0.25 for preform and top die and 0.30 with bottom die in lubricated condition. The friction factors for un-lubricated case are calculated as 0.50 for top die and 0.55 for bottom die. The difference of 0.05 in the friction factors between top and bottom is found to be effective in predicting the actual dimensions of the pressed cylindrical performs. Though the machine used is not very sensitive still the load recorded for height reduction matched well with the calculated load. From the trends of relative density

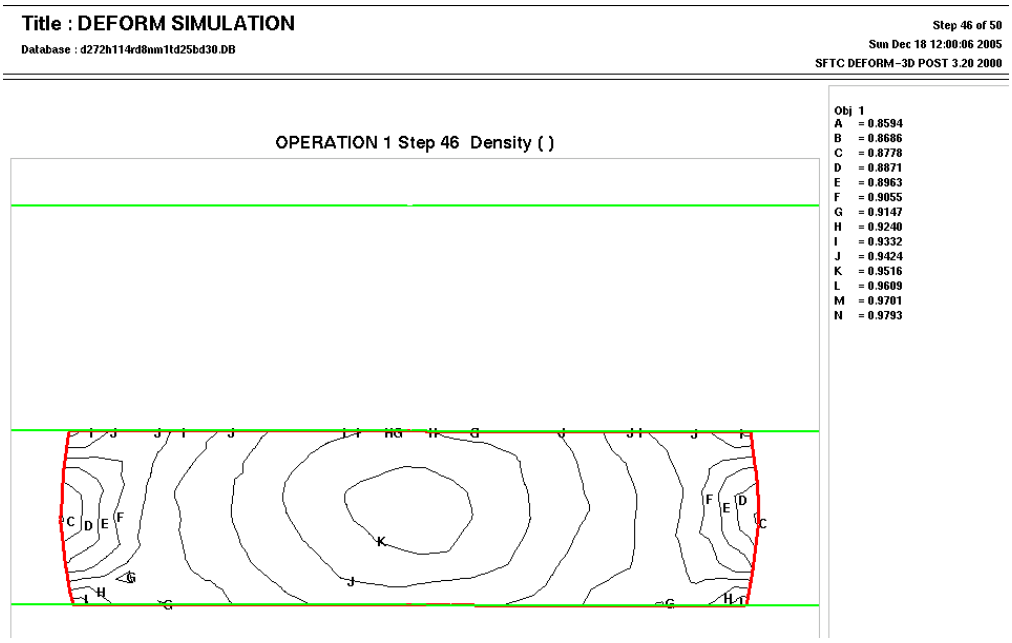

Fig.15. Density distribution of Cold Forged Preform obtained through Simulation.

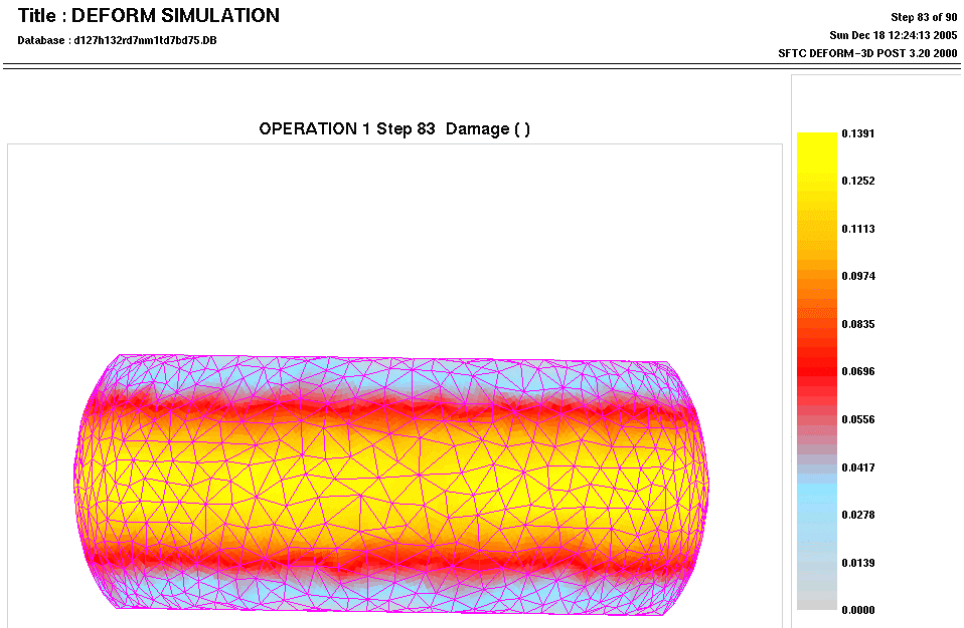

Fig.16. Probable damage area (with the rate of more susceptible to damage) of the Cold Forged Prefrom.

variation at different points in the pressed cylinder the crack prone areas can be effectively identified and necessary precautions can be taken accordingly.

ACKNOWLEDGEMENT

Authors thankfully acknowledge the Vice-Chancellor of Jadavpur University for Financial assistance under 'Seed Support' of Potential for Excellence Scheme in carrying out the experimental part of this work and the Director, NIFFT, Ranchi, Jharkhand for providing the necessary infractural facilities in carrying out the Simulation of the above experiments, otherwise the work could not be given the present shape.

Notations

b: perpendicular distance from center of the disc to the side

$\dot{\varepsilon}_x, \dot{\varepsilon}_y, \dot{\varepsilon}_z$: principal strain increments
h: thickness of the specimen
k: constant equals to 2
n: constant quantity
L: die load
p: average pressure at the die/work piece interface
S: surface of velocity discontinuity
V: volume of the zone of plastic deformation
η : constant, a function of ρ only
ρ_0: dimensionless, ρ_r/ρ^*
ρ_r: real density of real contact area
ρ^*: apparent density of the apparent contact area
τ: shear stress
φ_0: specific cohesion of the apparent contact area
μ: co-efficient of friction
σ_0 : yield stress of the non-work hardening matrix metal
J^* : External power supplied

REFERENCES

David, Dr., Zener, C. and Cai, Haimain. 1998. Common Causes of Cracks in Powder Metallurgy Compacts. The International Journal of Powder Metallurgy. 34 (4): 33-52.

Deryagin, BV., Izd. Akad. and Nauk. 1952. USSR.

German, RM. 1994. Powder Metallurgy Science, 2nd edition, Powder Metallurgy. Industries Federation, Princeton, NJ, USA.

German, RM. 1990. Powder Packing Characteristics, Metal Powder Industries Federation, Princeton, NJ, USA.

Haglund, S. and Agren, J. 1988. W content in Co binder during sintering of WC-Co. Acta Metall.46: 2801.

Ibhadode, AOA. 1989. Simulation and experimental verification of completely closed cavity die forging on a mechanical press. Journal of Engineering Manufacturing. 30: 17-32.

Im, YT. and Kobyashi, S. 1985. FE analysis of plastic deformation of porous Materials in Metal Forming and Impact Mechanism' Pergamon Press, Oxford, UK. pp 103.

Im YT. and Kobayashi. S. 1986. Analysis of Axisymetric Forging of porous materials by FEM'. Adv. Manufacturing Processes, Vol.1, pp.473.

Mori, K., Shima.S. and Sakada, KO. 1980. Finite Element Method for the analysis of Plastic Deformation in Porous Metals' Bulletin of JSME. 23 (178): 516.

Oh, SI., Wu, WT. and Park, JJ. 1987. Application of the Finite Element Method to P/M forging processes, Proceedings of 2nd ICPT, Stuttgart, West Germany. pp 961.

Oozo, K. and Yang, G. 1992. Application of Networks to Expert System for Cold Forging. Machine Tool Manufacturing. 577- 587.

Ramakrishna, P. 1980. Forging of Metal Powder Perform. Proceedings of the International Seminar on Metal Working Technology Today and Tomorrow. Ranchi, India.

Rooks, BW. 1974. The effect of die temperature on metal flow and die wear during high-speed hot forging, 15th Int. MTDR Conf., Birmingham, UK. Macmillan. London. pp 487.

Shama, S., Mahesha, S, Pavanachand, C., Rengarajan, R., Ramesh Rao S. 2002. Modeling Liquid Phase Sintering of Hard Metal Powder Compacts. PM^{2}TEC World Congress on Powder Metallurgy and Particulate Materials.

Sutradhar, G., Jha, AK. and Kumar, S. 1994. Production of sinter-forged components. Journal of Materials Processing Technology. 41: 143-169.

Sutradhar, G., Jha, AK. and Kumar, S. 1995. Cold Forging of Sintered Polygonal Discs. Journal of Institute of Engineers (India), Nov. 76: 148-152.

Tabata, T., Masaki, S. and Hosokawa, K. 1980. Int. J. Powder Metallurgy Powder Tech. 16, p.149.

Vedis, WV. and Geiling, KR. 1981. Relationship between Mechanical Properties and Particle Size on Iron Powder Compacts. The International Journal of Powder Technology. 17(2): 135.